Featured Articles

First-principles Materials-simulation Technology

Yuji Suwa, Ph.D.

Masakuni Okamoto, Ph.D.

Tomoyuki Hamada, Dr. Eng.

OVERVIEW: First-principles materials-simulation technology guides and assists the development of functional materials by high-precision calculations of electronic states. The accurate determination of electronic states is an important basis for understanding the mechanisms by which material functions come about so that their performance can be improved. It also enables theory-based materials design by predicting the functions of unknown materials. This article describes three current areas of work that use this technology, namely predicting the efficiency of germanium light sources for "photonics-electronics convergence systems," the development of techniques for predicting the Curie temperature in the design of magnetic materials able to function at high temperature, and the development of highly efficient analysis techniques for strongly correlated materials that are difficult to analyze using standard methods.

INTRODUCTION

MATERIALS technology is an important field of technology that underpins innovation at Hitachi. While developing new materials is not easy, improving the performance of these materials or providing them with new functions can make a major impact, because they form a core part of numerous products and services.

In research aimed at enhancing the functions of materials, it is important to proceed on a basis of understanding the basic mechanisms by which those functions (physical properties) come about. At the cutting edge of development, it is not uncommon for the newness of materials to render existing knowledge irrelevant, and yet it is this that offers the key to higher performance.

To understand new materials, it is important first to determine their electronic states. Most material properties are a consequence of the behavior of electrons. This applies not only to electrical properties, such as whether the material is a metal, a semiconductor, or an insulator, but also such characteristics as melting point, boiling point, modulus of elasticity, and chemical reactivity. Optical and magnetic functions can also be explained in terms of electronic states.

First-principles calculation (simulation) is an essential tool for determining these electronic states. This method uses quantum mechanics (first principles) as the sole basis to calculate electronic states, without resorting to empirical parameters determined by experiment. Electronic states are calculated entirely from the atomic species and their positions. If necessary, the positions of atoms can be determined by searching for minimum-energy configurations. Because no empirical parameters are necessary to obtain results in agreement with experiments, even unknown materials that do not yet exist can be calculated with confidence. That is, first-principles calculation can be used not only to understand existing materials, but also as a valuable tool for theoretical materials design tasks, such as predicting the physical properties of unknown materials in advance of experiment, narrowing down promising candidate materials, and predicting optimal composition.

While a wide range of calculation methods fall under the term "first-principles calculation," density functional theory (DFT), which is based on the calculation of electron density distributions, is widely used because of its speed and accuracy. In fact, the term "first-principles calculation" is often synonymous with DFT. This section describes research that is based on DFT.

Although first-principles calculation technology is known to be useful, there is still a problem that even DFT, one of the fastest methods in first-principles calculations, imposes high computational costs, making it difficult to apply to computational models

that simulate a large number of atoms. This has led to problems such as an inability to calculate systems that require a large model or a loss of accuracy due to use of an oversimplified model. However, with computing hardware continuing to improve in speed by a factor of around 1,000 every decade[1], calculations are now much faster than they were 10 or 20 years ago. Together with advances in computational algorithms designed to take advantage of computer architectures with higher degrees of parallelism, this means that it is now possible to use much larger models. This has considerably expanded the range of phenomena that can be simulated, with the result that first-principles simulation is playing an increasingly important role in materials research.

At the Advanced Research Department, Central Research Laboratory, Hitachi, Ltd., first-principles simulation is used for research into a wide range of materials, including magnetic materials, lithium battery materials, light-emitting materials, thermoelectric materials, catalysts, and polymers. Because it is the novelty of a computational model or calculation method that provides new knowledge, research into these materials at Hitachi includes continually working to improve and extend simulation techniques to expand the range of phenomena that can be simulated and to improve accuracy.

This article describes such research into light-emitting materials, magnetic materials, and strongly correlated materials

EFFICIENCY PREDICTION FOR GERMANIUM LIGHT SOURCES

Use of optical wiring is one way to improve the performance and power consumption of silicon devices. The best way to achieve this at low cost is to develop a "photonics-electronics convergence system" (system that combines both photonics and electronics) in which light sources are fabricated on a silicon substrate using monolithic integration. Unfortunately, it is difficult to fabricate group III-V compound semiconductors, a well-known light source material, using the processes used in silicon chip manufacturing. Although the group IV element germanium has a good affinity with silicon processes, it suffers from a low light emission efficiency. This section describes the prediction of germanium light emission efficiency, which is part of the effort being made to overcome this difficulty so that germanium can be turned into a practical new light source material.

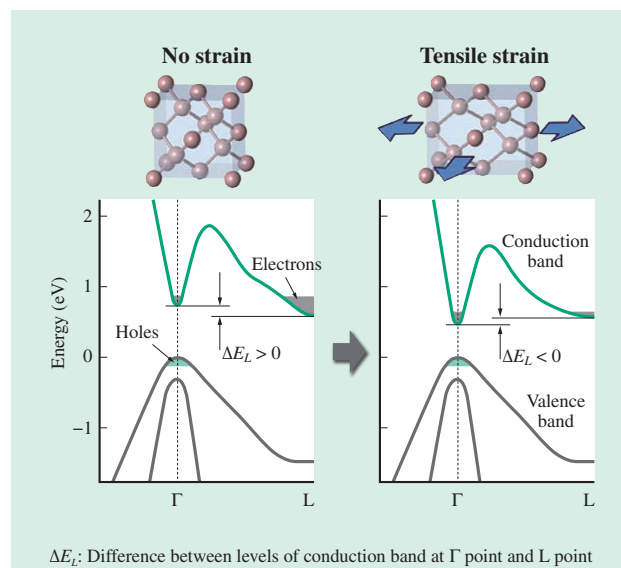ΔE_L: Difference between levels of conduction band at Γ point and L point

Fig. 1—Effect of Strain on Band Structure of Germanium. When strain is not present, germanium is an indirect-gap semiconductor with the L point as the lowest point of the conduction band. When a large strain is present, germanium becomes a direct-gap semiconductor with the Γ point becoming the lowest point.

Germanium is an indirect-gap semiconductor (see Fig. 1). The injection of current causes an accumulation of electrons at the bottom of the conduction band and holes at the top of the valence band. When there is an unoccupied state (a hole exists) in the valence band immediately below the conduction band electron, that electron can fall into that valence-band state (undergo a direct transition) by emitting a photon. In normal germanium, holes accumulate at the Γ point and electrons at the L point. Accordingly, light emission efficiency is low because these direct transitions do not occur, and instead light is only emitted by less frequent indirect transitions triggered by lattice vibration. On the other hand, it is known that the electronic state changes when tensile strain is applied, making it easier for electrons to accumulate at the Γ point, and that using a high concentration of n-type doping to provide a large number of electrons makes it possible to inject electrons not only at the L point but also the Γ point[2]. However, while simple qualitative predictions have been made for these effects, no quantitative predictions have yet been made. Because adequate light emission efficiency has yet to be achieved through experimental methods, Hitachi set out to use first-principles calculations to predict light emission efficiency so that this could be used in materials design to assess the extent to which strain and doping should be used.

Calculation of Light Emission Efficiency

This calculation method is based on the DFT using plane wave basis for describing wave function and pseudopotential method, which treats the nucleus and core orbital electrons as an ion core. A hybrid functional[3] is used as the exchange-correlation term.

The top of Fig. 2 shows the wave function for the Γ point of germanium. The blue and white surfaces are isosurfaces for the wave functions of the valence and conduction bands, with the different colors representing opposite signs. To determine the light emission efficiency, it is necessary to calculate the probability of optical transition between these two levels. This in turn requires obtaining the optical transition matrix elements. That can be calculated by applying the x, y, and z partial differential operators to one of the wave functions, multiplying this with the other wave function and integrating the product.

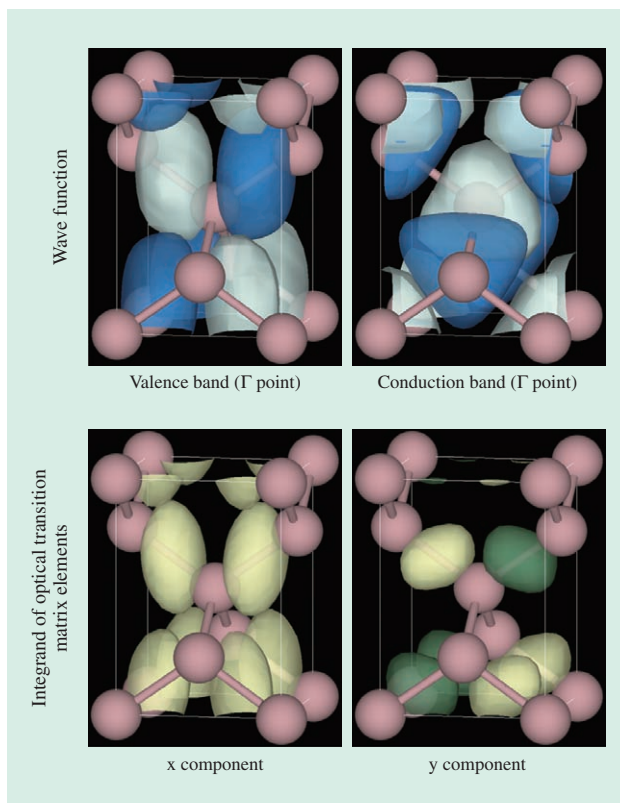The bottom half of Fig. 2 shows the distribution of this integrand. The different colors represent opposite signs. This shows that a non-zero value remains for the x component after performing a spatial integration, but that the positive and negative contributions for the y component cancel to zero. This indicates that a transition between these two states is only possible with the emission of light polarized in the x direction. The light emission efficiency can be obtained by performing this calculation for all combinations of electronic states between which transitions are possible and summing them with reference to the occupation of electrons and holes.

Although there is a difficulty in the calculation of optical transition matrix elements using a plane-wave based pseudopotential method by which considerable error arises in the core region, it was solved by incorporating a core-repair term[4, 5] and the calculation was kept accurate.

Prediction of Light Emission Efficiency for Germanium Under Strain

The factors that have a major influence on the light emission efficiency of germanium are the injected electron density, hole density, strain, density of crystal defects, and temperature. Fig. 3 shows the calculated result of optical gain for an ideal defect-free germanium crystal at room temperature (300 K) using the electron and hole densities as parameters.

Achieving lasing is an important requirement for obtaining sufficient light output for use as a light source in photonics-electronics convergence systems,
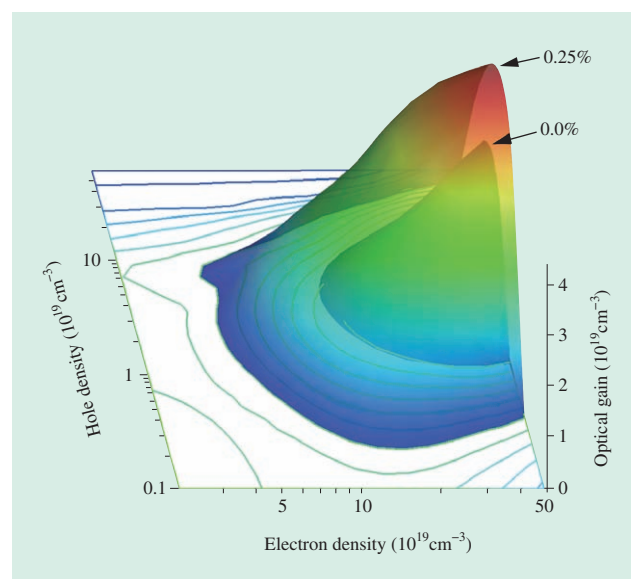
Fig. 2—Germanium Wave Function and Calculation of Optical Transition Matrix Elements.
The different colors of the isosurface represent opposite signs. The higher the optical transition matrix elements calculated from the valence band and conduction band wave functions, the higher the light emission efficiency.

Fig. 3—Calculated Result of Optical Gain.
The results are for no strain (0.0%) and for a biaxial strain (0.25%) parallel to the (001) plane. The gain is negative in regions where no colored surface is shown.

and to realize that, the optical gain of the light-emitting material should be positive. If there are wavelengths at which the net gain (after subtracting the light absorption loss from the light emission efficiency) is positive, lasing is possible at those wavelengths. Fig. 3 also shows the calculated net gains for the cases of no strain and 0.25% biaxial tensile strain parallel to the (001) plane where the vertical coordinate of the surfaces represents the gain (only shown for positive values). Regions where no surface is shown have a negative gain. The figure indicates that a positive gain is available at lower electron and hole densities when strain is present. Put another way, the presence of strain results in a higher gain for the same carrier (electron or hole) density. Looking at the locations where the surfaces are shown also indicates that the minimum necessary electron density is always much larger than the minimum necessary hole density. This is a consequence of the fact that electrons are not injected at the Γ point until they have filled up the region around the L point.

Although inversion of the Γ point and L point levels does not occur until a large strain of about 1.5% is present, as shown in Fig. 1, Fig. 3 indicates that gain improvement can be achieved at a comparatively easily achieved strain of 0.25% by reducing the difference between the two levels. Although positive gain regions also exist when no strain is present, these require impractically high electron densities of about 10^{20}cm^{-3}. Accordingly, taking advantage of strain to reduce the required density is a more realistic alternative.

While the above describes the calculation of gain at room temperature, heating due to the injected current raises the temperature in an actual device. Fig. 4 shows the gain at a variety of temperatures calculated to determine how the gain changes under such conditions. The figure shows the gains for a germanium crystal n-type doped with an electron density of $4.6 \times 10^{19} \text{cm}^{-3}$ and with a strain of 0.25% (same as Fig. 3) when the same number of electron and hole carriers are injected (current injection). Fig. 4 shows that, even if the temperature rises above 100°C (400 K), and the gain falls, there is still an adequate region with a positive gain. Also, because the gain region expands if the temperature falls, it demonstrates that cooling is a useful technique for experimental confirmation of lasing.

These results show that achieving a gain requires carrier injection on the order of 10^{19}cm^{-3}, a level of carrier density that is not easy to achieve. A small number of defects also inevitably appear during
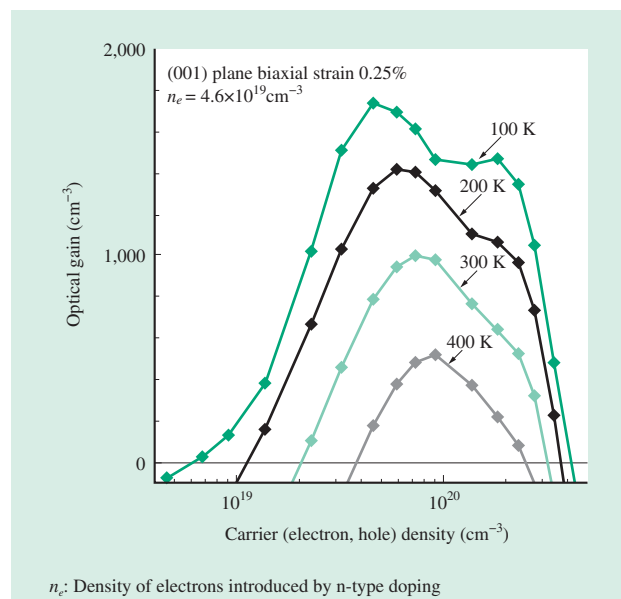

Fig. 4—Temperature Dependence of Optical Gain.
A region in which lasing can occur is still present even if the temperature increases by about 100°C from room temperature. Cooling significantly expands the conditions under which lasing occurs.

device manufacturing, reducing the crystallinity. These defects shorten the life time of the injected carriers and prevent increases in the carrier density. Because doping and the use of strain to increase light emission efficiency also increase defects, too much of these will have the opposite effect of reducing the light emission efficiency. To find the optimal balance of strain, doping, and crystallinity needed to achieve lasing by theoretical material design will be our next research subject.

FIRST-PRINCIPLES ANALYSIS OF THE CURIE TEMPERATURE OF MAGNETS

High-performance magnets are used in a number of familiar products, such as hybrid electric vehicles (HEVs), air-conditioning compressors, and hard disks. While neodymium magnets ($Nd_2Fe_{14}B$) are the most common type of ferromagnets in current use, their poor high-temperature properties mean they require the addition of dysprosium (Dy), a rare metal. However, there was a sudden disruption in supply of this material in 2010, and this created a need for the development of new high-performance magnets that do not use rare metals. A key point is being able to provide adequate magnetism at product operating temperatures. The operating temperature of an HEV, for example, is about 200°C (473 K) or

more. The key to determining the magnetism at non-zero temperatures is the Curie temperature, which needs to be sufficiently higher than the operating temperature. The following sections describe a technique developed by Hitachi for the theoretical prediction of Curie temperature.

Curie Temperature

The electrons in the iron (Fe) and other magnetic atoms present in a magnetic material impart a magnetic moment (spin) allowing the atoms to form a three-dimensional (3D) crystal lattice. Fig. 5 shows the concept behind this phenomenon. The quantum mechanical interaction between these spins causes them to align at low temperatures, forming a ferromagnetic state. At higher temperatures, the spins fall out of alignment, reducing the magnetism to zero (paramagnetic state). The temperature at which this transition occurs is called the Curie temperature (T_C).

Calculation Method

The Heisenberg model is used for the theoretical calculation of Curie temperature. In this model, the Hamiltonian for the energy of the system is written as follows:

$$H = -\sum_{ij} J_{ij} \mathbf{S}_i \cdot \mathbf{S}_j - \sum_i \mathbf{h} \cdot \mathbf{S}_i \qquad (1)$$

Where $\mathbf{S}_i$ and $\mathbf{S}_j$ are the spins (3D vectors) at sites i and j, and the exchange parameters J_{ij} determine the strength of interaction between them. These exchange parameters, which are the critical elements of this method, can be calculated from first principles with high precision. Specifically, the Liechtenstein method[6] that determines J_{ij} from the change in energy when the spins at sites i and j only are varied by an angle θ is used. In this case, Hitachi used the AkaiKKR[7] first-principles calculation (DFT) code to calculate J_{ij}. Once the Hamiltonian is determined, the spin states at non-zero temperatures can be determined from the statistical-mechanical partition function (Z).

$$Z = \sum_{\{\mathbf{S}_i\}} e^{-H/k_B T} \qquad (2)$$

Although it is necessary to use an approximation to calculate the partition function, Hitachi used the Monte Carlo method, which provides the highest level of accuracy. Hitachi also tried using mean field approximation, whereby the mean value of the spin is used to minimize the computational load. However, this proved to be impractical because it ignores the
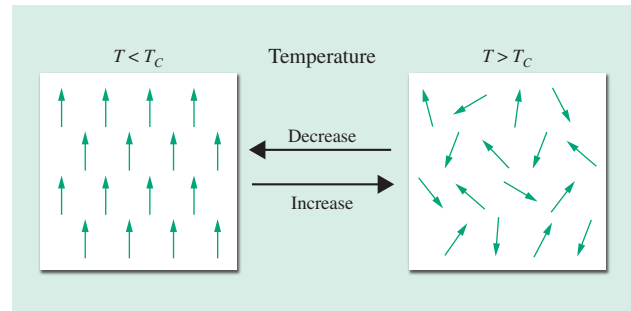

Fig. 5—Concept of Curie Temperature.
In a magnetic material, a lattice is formed by the magnetic moment (spin) of magnetic atoms. The spin orientations become aligned at low temperatures (ferromagnetic state) (left) but lose this alignment at higher temperatures (paramagnetic state) (right). The temperature at which this transition takes place is called the Curie temperature (T_C).
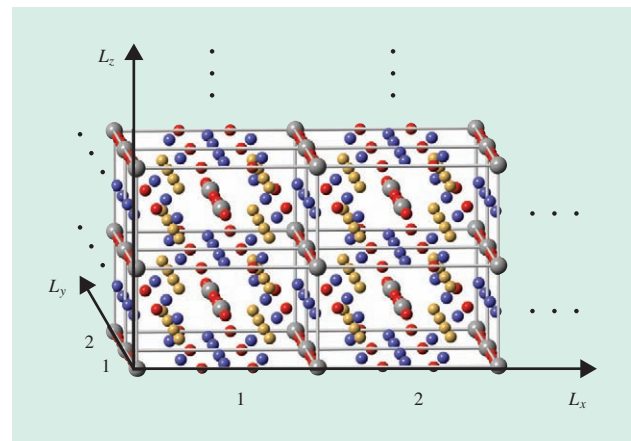

Fig. 6—Crystal Model.
The actual calculation is performed for a three-dimensional lattice consisting of $L_x \times L_y \times L_z$ unit cells (the figure shows tetragonal YFe_{12}). The correct result is obtained when the lattice size (L_x, L_y, L_z) is infinitely large.

effect of spin fluctuation and produces results that overestimate T_C by around 200 K to 300 K.

The Monte Carlo method uses random numbers for the spin orientation at points in a 3D lattice extending across $L_x \times L_y \times L_z$ (= N) unit cells to generate probabilistic variation (see Fig. 6). The larger the lattice size (L_x, L_y, L_z), the closer this approaches an actual system. While the Monte Carlo method gives a partition function that is more accurate than any other approximation, the problem with it is that, when used to calculate T_C directly, it requires that a sufficiently large lattice be used to approximate reality, and this increases the computational load. Accordingly, Hitachi resolved this lattice size problem by using a method that calculates a quantity known as a "4th order cumulant."

Solution to Lattice Size Problem

The 4th order cumulant (U_L) is defined as follows.

$$U_L = 1 - \frac{\langle M_z^4 \rangle}{3 \langle M_z^2 \rangle^2} \tag{3}$$

Here the lattice size is $L_x = L_y = L_z$ (=L). U_L has the property of being equal to zero when treated as a Gaussian distribution for which the mean value of the z-axis magnetization M_z ($= \Sigma_i S_{zi}/N$) is zero ($<M_z> = 0$). This condition is satisfied when the system is above the Curie temperature. Another property of U_L is that, at the Curie temperature, it is not dependent on the lattice size. When calculated for tetragonal yttrium-iron (YFe$_{12}$), for example (see Fig. 7), as L increases, U_L converges on one of the values $\frac{2}{3}$, 0.38, or 0 (fixed point U^*), depending on the temperature. Here, $\frac{2}{3}$ corresponds to the ferromagnetic state when $T = 0$, and 0 corresponds to the paramagnetic state when $T = \infty$. Similarly, 0.38 corresponds to the Curie temperature and in this case U_L clearly has little dependence on L. Although specifying the spin state at the Curie temperature is difficult, when all spins are aligned and have the same magnitude, and are then rotated at random, for example, the calculation gives $U^* = \frac{2}{5} = 0.4$. It is believed that the value of $U^* = 0.38$ comes abou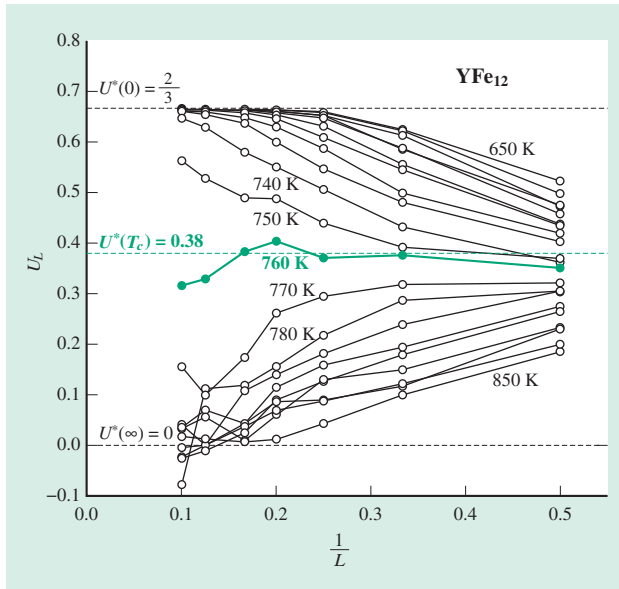t because short-range correlation states have the effect of reducing U^* by a small amount. These three fixed points are generally explained from a renormalization group perspective in terms of the relative magnitudes of the correlation length (ξ) of the magnetization (M_z) and the lattice size (L)[8]. Hitachi has taken advantage of this property to calculate the Curie temperature with high accuracy using a comparatively small lattice.

Testing on Common Magnets

The newly developed technique was used to calculate the Curie temperature of ferromagnetic materials such as body-centered cubic iron (bcc-Fe), body-centered cubic cobalt (bcc-Co), face-centered cubic nickel (fcc-Ni), YFe$_{12}$, Y$_2$Fe$_{17}$, and yttrium-iron nitride (Y$_2$Fe$_{17}$N$_3$). Fig. 8 shows a plot of the results, with the vertical axis representing the calculated temperatures and the horizontal axis representing the measured values. The dotted line indicates agreement between the calculated and measured values. The calculations for bcc-Fe and bcc-Co, which have simple structures, match the measured values exactly. Meanwhile, although the calculation slightly overestimates the Curie temperatures for the complex structures of YFe$_{12}$, Y$_2$Fe$_{17}$, and Y$_2$Fe$_{17}$N$_3$, the calculated temperatures are in the same relative order as the measured values. The calculation underestimates the Curie temperature of Ni. This can be explained by the low magnetic moment of Ni, which means the Heisenberg model provides a poor approximation. That these calculations reproduce
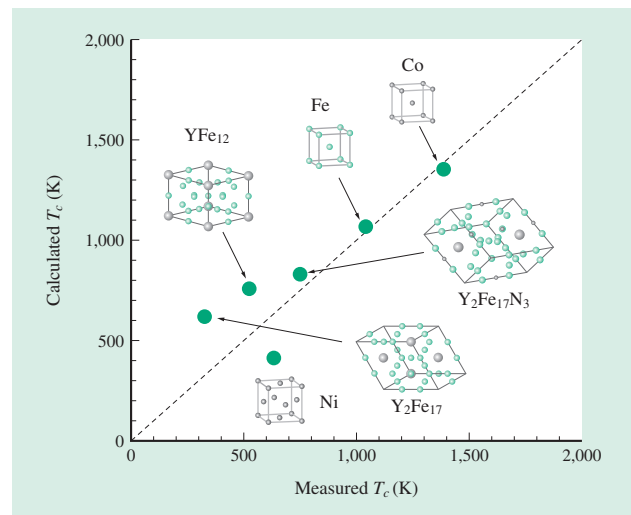

Fig. 7—Dependence of 4th Order Cumulant on Lattice Size.
As the size of the lattice used in the calculation (L) increases, the 4th order cumulant (U_L) converges on one of the fixed points (U^*) (0, 0.38, or $\frac{2}{3}$), depending on the temperature. The graph shows there is no dependence on L at the temperature that gives $U^* = 0.38$. This property can be used to obtain the Curie temperature ($T_C = 760$ K) with high accuracy.

Fig. 8—Curie Temperature of Common Magnetic Materials.
The graph plots the Curie temperature calculated for ferromagnetic materials by this method (vertical axis) against their experimental values (horizontal axis). The Monte Carlo calculation is in good agreement with experiment even for materials with complex structures (YFe$_{12}$, Y$_2$Fe$_{17}$, Y$_2$Fe$_{17}$N$_3$).

the measured values with a practical level of accuracy indicates that this technique can be used to predict the Curie temperature of new materials from first principles. Accordingly, the technique will be useful for developing a new generation of magnetic materials that do not use rare elements.

USE OF DFT + U METHOD TO ANALYZE STRONGLY CORRELATED MATERIALS

While the DFT method is recognized as suitable for analyzing the electronic states of most materials, there is one class of materials to which it is not applicable. That class consists of materials with localized electrons, what is known as a "strongly correlated electron system." In addition to the magnets described above, other examples of strongly correlated electron systems include the cathode material used in lithium-ion batteries, high transition temperature (high-Tc) superconductors, metal oxides, and catalysts. Since these materials play an important role in social infrastructure systems, analysis of the electronic structures of strongly correlated electron systems is an important topic for infrastructure materials research.

The DFT method uses the electronic states of a hypothetical system (in which there is no interaction between electrons) as the basis for analyzing actual electronic structures where interactions are present. Accordingly, while the DFT method is suitable for analyzing the electronic structures of materials such as semiconductors and metals with properties determined by free electrons, it is less suited to performing such analyses for strongly correlated electron systems with localized electrons. The solution to this problem with the DFT method is the DFT + U method[9], [10]. Fig. 9 shows an overview.
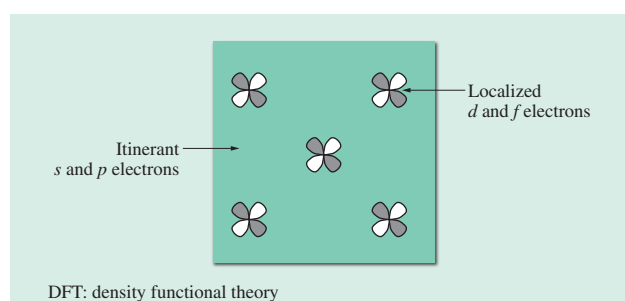

DFT: density functional theory

Fig. 9—Overview of DFT + U Method.
This strongly correlated electron system consists of itinerant s and p electrons and localized d and f electrons. The DFT + U method uses the DFT method for the s and p electrons and introduces the concept of on-site energy for the d and f electrons.

The electrons in a strongly correlated electron system can be divided into highly itinerant s and p electrons (electrons with s and p atomic orbital components) and highly localized d and f electrons (electrons with d and f atomic orbital components). The DFT + U method uses the DFT method for the s and p electrons and the approximate Hartree-Fock wave function method for the d and f electrons. The Hartree-Fock wave function method uses an approximation that only considers the on-site (within same atom) electronic interactions. Inter-atomic electronic interactions are ignored. Because consideration for the electronic interactions for d and f electrons is an inherent part of the DFT + U method, it can take appropriate account of their being localized and correctly specify the electronic states of a strongly correlated electron system.

Theoretical Determination of U_{eff}

The DFT + U method uses the effective interaction parameter (U_{eff}) for the on-site interactions between localized electrons. U_{eff} is obtained from the difference between the parameter for Coulomb interaction between electrons (U) and the exchange interaction parameter (J) ($U_{eff} = U - J$). U_{eff} is typically obtained empirically, and often takes a value of around 5 eV. However, use of an empirical value for U_{eff} is undesirable because it means the calculation is no longer from first principles and therefore confidence in it is undermined.

Accordingly, Hitachi set about performing first-principles DFT + U calculations in which U_{eff} was calculated theoretically. The constraint DFT method[11], [12] is recognized as one way to calculate a value for U_{eff} theoretically. This method performs the DFT calculation for different numbers of localized electrons in a strongly correlated electron system to obtain U from the second derivative of energy with respect to the number of localized electrons. This was done using the linearized muffin tin orbital method, which provides an easy way to calculate electronic structures for different numbers of localized electrons, rather than with the more accurate pseudopotential method. This is because it is difficult to use the pseudopotential method to calculate electronic structures for different numbers of localized electrons. To overcome this problem, Hitachi developed a technique for the theoretical calculation of U_{eff} in the DFT + U method based on the pseudopotential method[13]. This works by performing the DFT + U calculation for small variations in the value of U_{eff} around 0 eV and using the number of localized electrons and change in

energy given by this calculation to obtain the second derivative for energy with respect to the number of localized electrons, and thereby to calculate the value of U. Because the value of J can be approximated as $\frac{1}{10}$ the value of U[11], this can be used to determine $U_{eff} = U - J$. Because the value of U_{eff} obtained by this procedure does not include any empirical parameters, it means that the DFT + U calculation can be performed from first principles.

Electronic State Calculation for Antiferromagnetic Ce$_2$O$_3$ and Nd$_2$O$_3$

This section describes the application of the first-principles DFT + U method to cerium (III) oxide (Ce$_2$O$_3$) and neodymium (III) oxide (Nd$_2$O$_3$).

Ce$_2$O$_3$ is a catalyst for reducing exhaust emissions and Nd$_2$O$_3$ is a material that occurs in crystal boundaries in neodymium magnets and may influence their coercivity. Both have a hexagonal crystal structure and

constitute strongly correlated electron systems with localized *4f* electrons in their respective Ce and Nd atoms. Hitachi used the DFT + U method to calculate the electronic states, using the method described above to determine the values of U_{eff} for the *4f* electrons. The U_{eff} values are 8.99 eV for Ce and 8.17 eV for Nd. These values are larger than the empirical value of 5 eV. The generalized gradient approximation (GGA) was chosen as the exchange-correlation term in the DFT part of the calculation. The materials were also assumed to be in an antiferromagnetic state.

Fig. 10 and Fig 11 show the results of calculating the density of states (DOS) for Ce$_2$O$_3$ and Nd$_2$O$_3$ respectively. To compare the differences between calculation methods, the graphs show the results for both DFT on its own and DFT + U. DOS has both a positive and negative value, representing the up and down spin components. Because the material is in an antiferromagnetic state, there is little difference
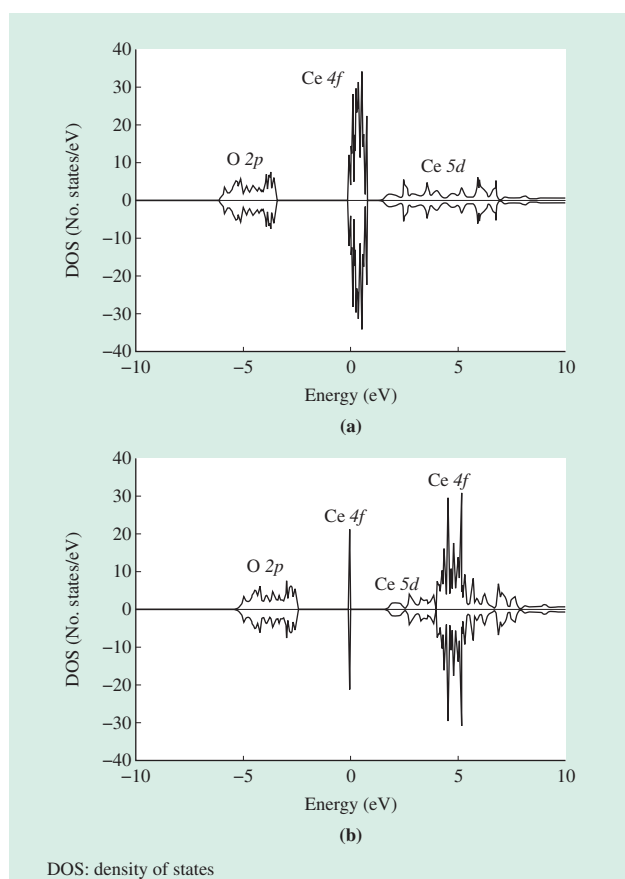

DOS: density of states

Fig. 10—Density of Electronic States for (Antiferromagnetic) Hexagonal Ce$_2$O$_3$.
Graph (a) shows the result calculated using the DFT method and graph (b) shows the result calculated using the DFT + U method. The DFT + U method gives a U_{eff} of 8.99 eV for the 4f electrons of Ce.
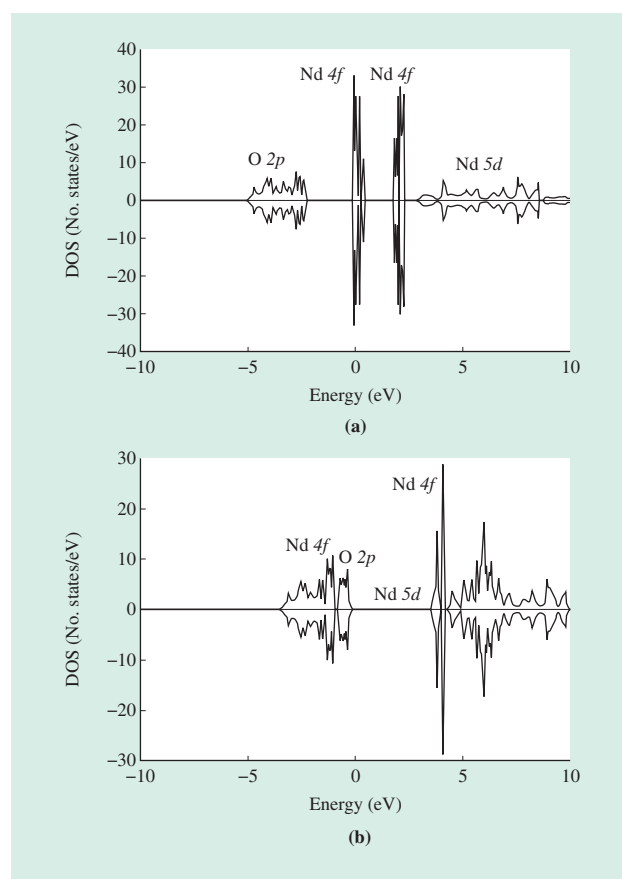
Fig. 11—Density of Electronic States for (Antiferromagnetic) Hexagonal Nd$_2$O$_3$.
Graph (a) shows the result calculated using the DFT method and graph (b) shows the result calculated using the DFT + U method. The DFT + U method gives a U_{eff} of 8.17 eV for the 4f electrons of Nd.

between spin components, giving a graph with horizontal symmetry.

States with an energy of 0 eV are at the Fermi level and the DOSs at and around these states have a major influence on the electrical behavior of the material. The results calculated using the DFT method show that both Ce_2O_3 and Nd_2O_3 have non-zero DOSs at and around 0 eV, and since there is no band gap (energy ranges where the DOS is zero) at these energy levels, the electronic states behave like a metal. As these materials are in fact insulators, this indicates that the DFT method has failed to reproduce experimental results. The DFT + U calculation, on the other hand, correctly reproduces experimental results by showing that both materials have a band gap at around 0 eV and therefore behave like insulators.

The size of the gap between the *2p* band (O) and *4f* band (Ce) for Ce_2O_3 calculated by DFT + U is 2.34 eV. This is very close to the measured value of 2.4 eV[14]. Similarly, the gap between the *4f* band (Ce) and *5d* band (Ce) is calculated to be 1.49 eV, which is close to the value of 1.29 eV calculated by the GW method[15] (which considers many body effects and therefore is accurate but with a high computational cost). When the same calculation is performed using an empirical value of U_{eff} (5 eV), it gives a band gap of 1.69 eV between the *2p* band (O) and *4f* band (Ce) and 2.19 eV between the *4f* band (Ce) and *5d* band (Ce), indicating poor agreement with the experimental values.

In the case of Nd_2O_3, the DFT + U method calculates a band gap of 3.44 eV, considerably different from the experimental value of 4.7 eV[14]. This is because the band gap for this material is determined by the energy difference between the *2p* band (O) and *5d* band (Nd). As U_{eff} is introduced for the Nd *4f* electrons, the *4f* band (Nd) is split into high and low energies and is away from the Fermi level. In contrast, there is no U_{eff} for bands such as the *2p* band (O) and *5d* band (Nd), and therefore these remain close to the Fermi level. It is known that the self-interaction of electrons gives the DFT method a tendency to underestimate the band gap, and the difference in level between the *2p* band (O) and *5d* band (Nd) is underestimated here for the same reason. Accordingly, introducing the U_{eff} for the Nd *5d* electrons also has the potential to improve the calculated value of band gap. Furthermore, when the DFT + U calculation was performed using an empirical value for the U_{eff} for the Nd *4f* electrons (5 eV), it indicated that the electronic states behave like a metal and failed to correctly describe the insulating nature of Nd_2O_3.

These results confirmed the reliability of a first-principles DFT + U method that uses theoretical calculations to determine U_{eff}, and that it has better agreement with experiment compared to past DFT + U methods that have determined U_{eff} empirically. This method, which can be used alongside the accurate pseudopotential method, and which can analyze the electronic states of strongly correlated electron systems at high speed and with a similar computational cost to the DFT method, is an effective tool for designing the strongly correlated materials that underpin social infrastructure systems.

CONCLUSIONS

A decade ago, it was predicted that the thousand-fold improvement in computer speed every 10 years would begin to slow down. In practice, no such slowing has occurred[1], and the trend can be expected to continue for some time yet. Accordingly, the scope and reliability of research based on the use of computer simulation will continue to grow in the future.

Although the value of first-principles calculation technology has already been demonstrated and is widely acknowledged, the details of this technology are not yet complete. Progress continues with a variety of improvements being achieved on a regular basis. Given this situation, if materials research is to be pursued using first-principles calculations to advantage, it is essential to follow up on advanced simulation technology continuously and to take up the challenge of making new improvements as described here. Hitachi intends to continue with these efforts in the future to expand the scope of research, and to work on elucidating the physical properties of new substances and on performing theoretical design of new materials.

ACKNOWLEDGEMENTS

REFERENCES

(1) TOP500 SUPERCOMPUTER SITES, http://www.top500.org/

(2) J. Liu et al., "Ge-on-Si Laser Operating at Room Temperature," Optics Letters **35**, pp. 679–681 (2010).

(3) C. Adamo et al., "Toward Reliable Density Functional Methods without Adjustable Parameters: The PBE0 Model," The Journal of Chemical Physics **110**, 6158 (1999).

(4) H. Kageshima et al., "Momentum-matrix-element Calculation Using Pseudopotentials," Physical Review B 56, 14985 (1997).

(5) Y. Suwa et al., "Intrinsic Optical Gain of Ultrathin Silicon Quantum Wells from First-principles Calculations," Physical Review, B 79, 233308 (2009).

(6) A. I. Liechtenstein et al., "Local Spin Density Functional Approach to the Theory of Exchange Interactions in Ferromagnetic Metals and Alloys," Journal of Magnetism and Magnetic Materials **67**, pp. 65–74 (1987).

(7) H. Akai, "Fast Korringa-Kohn-Rostoker Coherent Potential Approximation and its Application to FCC Ni-Fe Systems," Journal of Physics: Condensed Matter **1**, pp. 8045–8063 (1989).

(8) K. Binder, "Critical Properties from Monte Carlo Coarse Graining and Renormalization," Physical Review Letters **47**, pp. 693–696 (1981).

(9) N. Hamada, "Solid-state Physics," 43, pp. 743–749 (2014) in Japanese.

(10) V. I Anisimov, "Strong Coulomb Correlations in Electronic Structure Calculations: beyond the Local Density Approximation," Gordon and Breach Science Publishers (2002); Chapter 2.

(11) I. Solovyev et al., "t2g Versus All 3d Localization in LaMO3 Perovskites (M = Ti– Cu): First-principles Study," Physical Review B, 53, 7158 (1996).

(12) A. K. MacMahan et al., "Calculated Effective Hamiltonian for La2CuO$_4$ and Solution in the Impurity Anderson Approximation," Physical Review B, 38, 6650 (1988).

(13) T. Hamada, "Electronic State Calculation System and Program," Japanese Patent No. 5430665 (2013) in Japanese.

(14) A. V. Prokofiev et al., "Periodicity in the Band Gap Variation of Ln$_2$X$_3$ (X = O, S, Se) in the Lanthanide Series," Journal of Alloys and Compounds **242**, pp. 41–44 (1996).

(15) H. Jiang et al., "Electronic Properties of Lanthanide Oxides from the GW Perspective," Physical Review, B, 86, 125115 (2012).

ABOUT THE AUTHORS

Yuji Suwa, Ph.D.
Advanced Research Department, Life-science Research Center, Central Research Laboratory, Hitachi, Ltd. He is currently engaged in research into light-emitting elements using first principles and the order-N method. Dr. Suwa is a member of The Physical Society of Japan (JPS) and The Surface Science Society of Japan.

Masakuni Okamoto, Ph.D.
Advanced Research Department, Life-science Research Center, Central Research Laboratory, Hitachi, Ltd. He is currently engaged in research into magnetic materials using first-principles calculations. Dr. Okamoto is a member of the JPS and the American Physical Society, and is a visiting professor at Yokohama City University.

Tomoyuki Hamada, Dr. Eng.
Life-science Research Center, Central Research Laboratory, Hitachi, Ltd. He is currently engaged in research into battery materials using first principles and the order-N method. Dr. Hamada is a member of The Japan Society of Applied Physics and the American Chemical Society, and is a visiting professor at Toyohashi University of Technology.